Br J Dermatol 2023; **188**:396–406
https://doi.org/10.1093/bjd/ljac088
Advance access publication date: 17 November 2022

BJD
British Journal of Dermatology
Translational Research

Skin programming of inflammatory responses to *Staphylococcus aureus* is compartmentalized according to epidermal keratinocyte differentiation status

Kalum Clayton,[1] Daniel J. Holbrook,[1] Andres Vallejo,[1] Gemma Porter,[1] Sofia Sirvent,[1] James Davies,[1] Jenny Pople,[3] Fei Ling Lim,[3] Myron Christodoulides,[1] Marta E. Polak[1,2] and Michael R. Ardern-Jones[1,4]

[1]Clinical and Experimental Sciences, Sir Henry Wellcome Laboratories, Faculty of Medicine, University of Southampton, Southampton, UK
[2]Institute for Life Sciences, University of Southampton, Southampton, UK
[3]Unilever, Colworth Science Park, Sharnbrook, Bedford, UK
[4]Department of Dermatology, University Hospitals Southampton NHS Foundation Trust, Southampton, UK
Correspondence: Michael R. Arden-Jones. Email: m.aj@soton.ac.uk
M.E.P. and M.R.A.J. contributed equally.

Linked Article: Cichy *Br J Dermatol* 2023; **188**:314.

Abstract

Background Acute cutaneous inflammation causes microbiome alterations as well as ultrastructural changes in epidermis stratification. However, the interactions between keratinocyte proliferation and differentiation status and the skin microbiome have not been fully explored.

Objectives Hypothesizing that the skin microbiome contributes to regulation of keratinocyte differentiation and can modify antimicrobial responses, we examined the effect of exposure to commensal (*Staphylococcus epidermidis*, SE) or pathogenic (*Staphylococcus aureus*, SA) challenge on epidermal models.

Methods Explant biopsies were taken to investigate species-specific antimicrobial effects of host factors. Further investigations were performed in reconstituted epidermal models by bulk transcriptomic analysis alongside secreted protein profiling. Single-cell RNA sequencing analysis was performed to explore the keratinocyte populations responsible for SA inflammation. A dataset of 6391 keratinocytes from control (2044 cells), SE challenge (2028 cells) and SA challenge (2319 cells) was generated from reconstituted epidermal models.

Results Bacterial lawns of SA, not SE, were inhibited by human skin explant samples, and microarray analysis of three-dimensional epidermis models showed that host antimicrobial peptide expression was induced by SE but not SA. Protein analysis of bacterial cocultured models showed that SA exposure induced inflammatory mediator expression, indicating keratinocyte activation of other epidermal immune populations. Single-cell DropSeq analysis of unchallenged naive, SE-challenged and SA-challenged epidermis models was undertaken to distinguish cells from basal, spinous and granular layers, and to interrogate them in relation to model exposure. In contrast to SE, SA specifically induced a subpopulation of spinous cells that highly expressed transcripts related to epidermal inflammation and antimicrobial response. Furthermore, SA, but not SE, specifically induced a basal population that highly expressed interleukin-1 alarmins.

Conclusions These findings suggest that SA-associated remodelling of the epidermis is compartmentalized to different keratinocyte populations. Elucidating the mechanisms regulating bacterial sensing-triggered inflammatory responses within tissues will enable further understanding of microbiome dysbiosis and inflammatory skin diseases, such as atopic eczema.

What is already known about this topic?

- The microbiome exists as a dynamic feature alongside host epidermal responses aimed at maintenance of commensal species and clearance of pathogenic species.
- During acute cutaneous inflammation in diseases such as atopic eczema there are alterations in the microbiome, as well as histological and ultrastructural changes to the stratified epidermis that disturb host–microbe interactions.

Accepted: 5 November 2022

What does this study add?

- Using patient-derived *ex vivo* biopsies alongside parallel bulk and single-cell transcriptomic and secreted proteomic profiling of epidermal models, this investigation suggests that pathogen-associated remodelling of the epidermis is compartmentalized to different keratinocyte populations.
- Single-cell transcriptomic analysis distinguished cells from basal, spinous and granular layers, which could further be distinguished in relation to model exposure, with important implications for long-term epidermal health and microbiome handling.

What is the translational message?

- Features of diseases such as atopic eczema are acute inflammation, microbiome alterations and epidermal ultrastructural changes.
- Heterogeneous perturbation of undifferentiated keratinocytes to dysbiosis indicates nontransient responses that may persist after pathogen clearance. However, unaffected basal keratinocytes remain, providing a target for epidermal homeostasis.
- Elucidating the molecular mechanisms regulating bacterial sensing-triggered inflammatory responses within tissues will enable increased understanding of the links between microbiome dysbiosis and inflammatory skin diseases.

The stratified epidermis maintains cutaneous homeostasis by mediating keratinocyte turnover, stratum corneum formation, microbiome handling and antimicrobial defence. Keratinocytes progress through the epidermis forming distinct basal, spinous, granular and cornified strata. Terminal differentiation of outer-layer keratinocytes forms the epidermal cornified barrier, eventually shed by desquamation, and constant tissue renewal by proliferation and differentiation is critical for skin function.[1] However, precisely if or how epidermal differentiation is modified by skin microbiome changes is not yet fully characterized.

Keratinocytes interact with the innate and adaptive immune systems.[2–4] Their primary role favours tolerance, dampening inflammation in the context of a healthy skin microbiome.[5] *Staphylococcus epidermidis* (SE) is a ubiquitous cutaneous colonizer and is almost always nonpathogenic. SE-induced immune training and dampening arise, in part, via host Toll-like receptor (TLR)3 sensing of bacterial products such as lipoteichoic acid and LP78.[6,7] However, *Staphylococcus aureus* (SA) can be highly pathogenic, but it mostly transiently colonizes human skin, being found on approximately one-third of the population.[8]

Keratinocyte sensing of SA by pattern recognition receptors such as TLR2 and TLR9, and nucleotide-binding oligomerization domain-containing protein 1 (NOD1) and NOD2, leads to inflammatory responses, notably dysregulated in atopic skin.[9] These are partly a host defence mechanism. TLR2-mediated activation of nuclear factor-κB transcription pathways induces expression of human β-defensin (hBD)3 and RNase7.[10] SA dominates the microbiota of lesional skin of atopic eczema, and significantly alters immune signalling, leading to more severe disease. Indeed, SA density correlates with disease severity, and lesion resolution associates with microbial clearance.[11]

Understanding the programming of the regulatory-versus-immunostimulatory axis in the skin is of great interest. We hypothesized that functional differences in keratinocyte differentiation arise from challenge with commensal or pathogenic bacteria. Addressing this, we utilized a three-dimensional epidermis culture, allowing investigations of the effects of bacterial colonization on keratinocytes at different states. Alterations of transcriptional programmes were captured by measuring gene expression by microarray and single-cell DropSeq RNA sequencing.[12]

Materials and methods

Patient samples

Explant skin tissue was donated from discard surgery and was consented under ethical approval (LREC number 07/Q1704/46). The explant skin tissue was placed epidermis down on agar plates spread with 10^6 colony-forming units (CFU) of bacteria and cultured overnight. Inhibition zones were calculated using ImageJ (https://imagej.nih.gov/ij).

Explant biopsy inhibition assay

Discarded skin was obtained from surgery, stored in phosphate-buffered saline (PBS) and further washed in fresh PBS before being punched to 8-mm biopsies and placed epidermis down on bacteria-inoculated agar plates followed by overnight incubation (Figure S1; see Supporting Information). Staphylococcal inhibition was determined by calculation of the zone of inhibited growth on agar plates from five skin biopsy donors, with three or six replicates per donor (Figure S2; see Supporting Information).

Reconstituted human epidermis models

Primary keratinocytes were seeded in culture inserts (Millicell, 0.4-μm pore size, 12-mm diameter; Merck Millipore, Watford, UK) to confluence for 48–72 h. For differentiation, culture media was replaced with KGM2 with 2% fetal bovine serum (FBS) and 1.8 mmol L^{-1} $CaCl_2$ (Sigma, Poole, UK). Air–liquid interface cultures were generated over 14–15 days.

Bacterial challenge

Staphylococcal strains used were SA (NCTC number 8325-4) and SE (ATCC number 12228).[13,14] Bacterial challenge was performed by adding 100 μL of either PBS, SA or SE (1×10^7 CFU mL^{-1} in PBS) to the model's apical aspect. Models were incubated for 3 h, washed in PBS and returned to incubate for a further 21 h.

Undernatant proteome profiling

The Proteome Profiler Human XL Cytokine Array Kit (R&D Systems Inc., Minneapolis, MN, USA) was used to

semiquantitatively assay undernatant media. ImageJ was used to measure the relative spot intensity, and duplicates were averaged for each analyte. Results of $<10\%$ of the maximum intensity were considered background signal.

Microarray analysis of epidermal models

Model RNA was obtained by addition of RLT lysis buffer (Qiagen, Hilden, Germany) and purified using the RNeasy Plus Mini Kit (Qiagen) using the manufacturer's instructions. The quality of purified RNA was assessed by Agilent 2100 Bioanalyzer using the RNA 6000 Nano Kit (Agilent, Santa Clara, CA, USA).

The SurePrint G3 Human Gene Expression v3 8×60K Microarray Kit (Agilent) was used for bulk transcriptomic analysis following all of the manufacturer's instructions. The numerical expression data of each array were acquired by the feature extraction software, and further analysis was performed in GeneSpring v14.9 (Agilent) and Ingenuity Pathway Analysis software (Qiagen).

CIBERSORT analysis of model composition

Models were assessed by *in silico* quantification for consistent epidermal stratification from bulk microarray data using CIBERSORT[15] (performed online at https://cibersort.stanford.edu). Reoptimization for CIBERSORT deconvolution of skin and epidermis was previously done by us.[16] The LM22 reference panel was replaced by data from Cheng *et al.*[17] Single-cell basal, mitotic and spinous keratinocyte data from healthy trunk skin were collapsed to pseudobulk profiles by gene-wise summation to provide reference signatures. All run settings were kept at default.

Single-cell RNA sequencing analysis

Single-cell RNA analysis was carried out as per DropSeq. Models were dissociated to suspension using TrypLE Express (Thermo Fisher Scientific Inc., Waltham, MA, USA). Briefly, 1 mL precooled TrypLE Express and 500 μL prewarmed TrypLE Express were added into the inserts for 15 min, then 1 mL cold PBS with 10% FBS was added. Cells were collected after 70-μm filtration, centrifugation and resuspension in fresh KGM2.

Models from the same challenge condition were pooled to reduce intermodel variation. Multiplexing across challenge conditions was achieved by tagging cells with barcoded antibodies following the Cell Hashing protocol.[18] Control samples were tagged with TotalSeq-A0251 (GTCAACTCTTTAGCG), SA samples with TotalSeq-A0252 (TGATGGCCTATTGGG) and SE samples with TotalSeq-A0253 (TTCCGCCTCTCTTTG). The DropSeq co-encapsulation with primer-coated microbead procedure was followed. After droplet breakage and microbead purification, cDNA libraries were generated as detailed previously.[19,20] Sequencing was performed on an Illumina NextSeq (Illumina, San Diego, CA, USA) using a paired-end run of $3.6–5.0\times10^4$ reads per cell, at the Wessex Investigational Sciences Hub laboratory, University of Southampton, UK.

Data preprocessing and bioinformatic analysis

Illumina-generated base call (BCL) files were converted to fastq using the bcl2fastq tool. The resulting read files were aligned using Kallisto (v.0.46.1) and Bustools (v.0.39.3) (https://www.kallistobus.tools).

Transcriptomic data from single-cell RNA sequencing were analysed, unless otherwise stated, using the python-based Scanpy framework (v1.4.6).[21] Quality control covariates were established such as removal of empty barcodes (EmptyDrops),[22] counts per cell, genes per cell and percentage of mitochondrial genes. Expression data were normalized by SCRAN.[23]

Sequencing batches were integrated using the batch-balanced *k*-nearest-neighbour method (BBKNN).[24] The data were visualized by scatter plot in the reduced dimensional space from Uniform Manifold Approximation and Projection (UMAP). Calculation of embedded density was performed to aid selection of the clustering resolution for optimal explanation of the granularity in cell biology. Leiden clustering was performed using a resolution of 0.5 for the whole dataset and a resolution of 0.2 on a restricted subset to properly reflect differences observed from bacterial challenge.[25]

Layer-defining epidermal makers were used for annotation of basal (*KRT5*, *KRT14*, *COL17A1)*, spinous (*KRT1*, *KRT10*) and granular layers (*KRT6A*, *KRT6B*, *KRT16*, *S100A7*, *S100A8* and *S100A9*). Differential gene expression analysis was performed using MAST (Benjamini–Hochberg *P*-value <0.01, $|\log FC|>1$).[26] Gene ontology analysis was undertaken using the tool ToppFun within the ToppGene suite (https://toppgene.cchmc.org).

Results

Epidermal models (Figure 1a) were processed for bulk RNA sequencing. Computational deconvolution by CIBERSORT confirmed that the models were highly stratified and consistent (Figure 1b). Modelled keratinocyte populations comprised approximately 90% cells of human epidermis, excluding the nonkeratinocyte populations (Figure 1c).

Epidermal inhibition of bacterial growth is species specific

To examine skin antimicrobial action, we cultured human skin explant models on agar plates with bacterial lawns. Growth inhibition rings for SA were significantly larger than for SE, indicating species-specific regulation by secreted factors (Figure 2a; and Figure S2).

We next investigated the effect of archetypal pathogenic and commensal staphylococcal infection of established epidermal models after 24 h. Models were challenged with either SA or SE at 10^2 or 10^6 CFU each, and bacterial growth was measured at 3 h and again at 24 h. Both bacterial species indicated similar bacterial CFU at 24 h postchallenge regardless of initial inoculation; however, SE showed greater proliferation (Figure 2b). The time course confirmed active inhibition of SA from either inoculum to similarly low levels ($P>0.99$) (Figure 2c, red). In contrast, both SE challenge doses demonstrated proliferation to similar levels at 24 h ($P=0.93$) (Figure 2c, blue), indicating that epidermal colonization is tolerated at around 10^8 CFU per model.

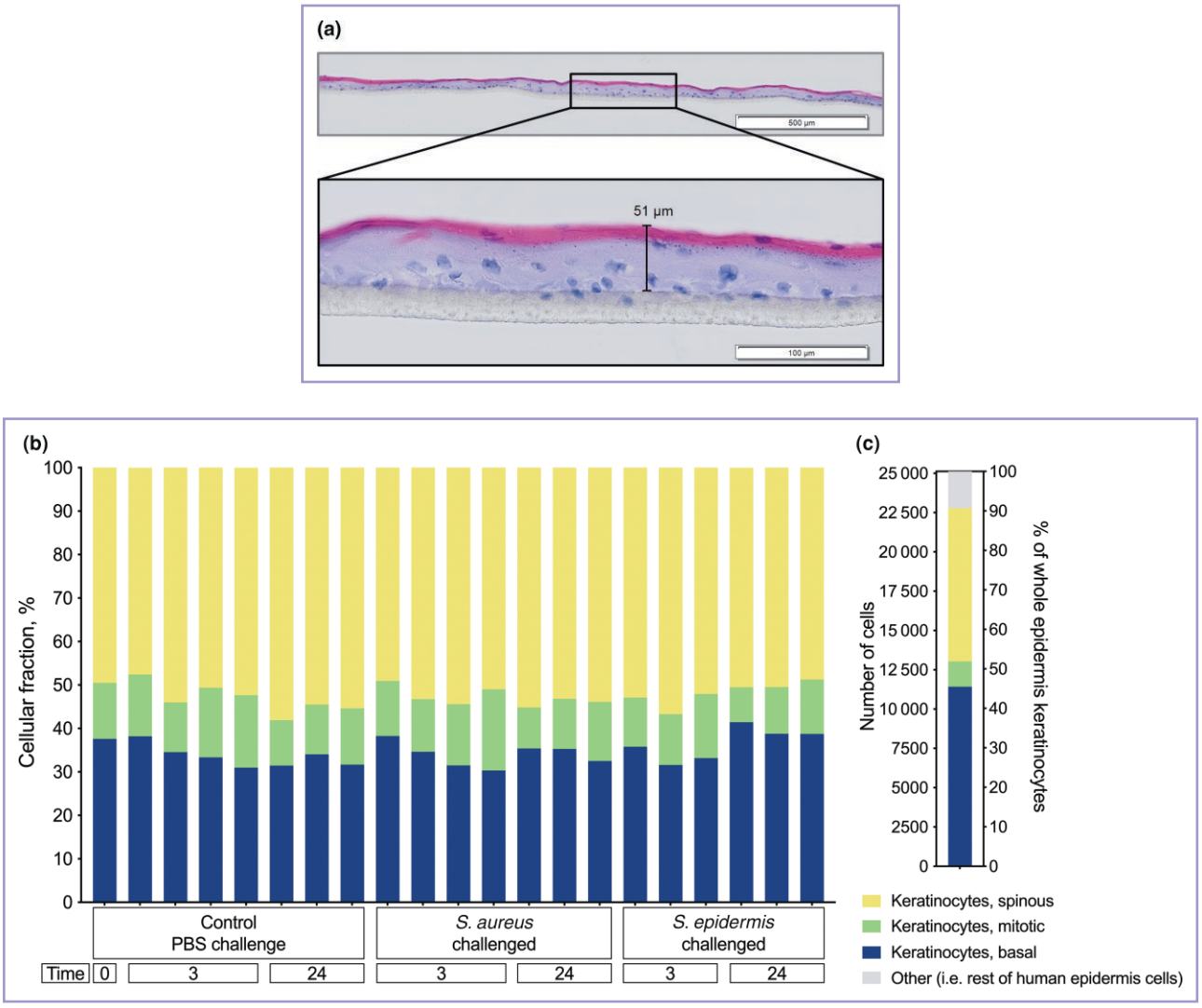

Figure 1 Reconstituted human epidermis (RHE) model culture. (a) Representative haematoxylin and eosin staining of an RHE model after 14 days of cultivation showing general morphology (top) and histology (bottom). (b) Twenty-one models were analysed by bulk microarray analysis and were subsequently resolved into relative basal (blue), mitotic (green) and spinous (yellow) populations using machine-learning deconvolution. PBS, phosphate-buffered saline. (c) Basal, mitotic and spinous populations for the deconvolution panel were derived from single-cell analysis of 25 000 keratinocytes from three samples of healthy human epidermis. These three populations comprising 100% of the *in vitro* models were composed of 90% of the cells isolated and annotated from healthy human epidermis.

Differential epidermal response to staphylococcal colonization is caused by altered expression of keratinocyte-derived factors

We hypothesized that epidermal inhibition of SA may derive from antimicrobial peptides (AMPs). Therefore, the key cutaneous AMPs were analysed from bulk transcriptomic analysis of skin models. Surprisingly, SA colonization did not significantly alter model expression of key AMPs at 24 h compared with naive controls, except for S100A15 (Figure 3a). In contrast, SE induced expression of the genes encoding LL-37, RNase 5, S100A8, S100A15, hBD2, hBD3 and hBD4 relative to control ($\log_2$ fold change >1) at 24 h (Figure 3a).

We reasoned that SA inhibition may derive from immune cell recruitment and activation via keratinocyte-derived cytokines, chemokines and growth factors. To explore immune-related soluble factors synthesized by keratinocytes in response to bacterial exposure, culture undernatants from bacteria-challenged models were harvested for proteomic analysis of 101 analytes (Figure S3; see Supporting Information). SA-challenged models showed dominantly proinflammatory mediators compared with naive controls, including CD14, CD30, GROα, interleukin (IL)-16 and vascular endothelial growth factor (Figure 3b).

Single-cell sequencing of epidermal models revealed stratified responses to staphylococcal challenge

To address our primary objective to characterize bacterial responses within epidermal strata, we generated a single-cell RNA sequencing dataset from naive control, SE-challenged

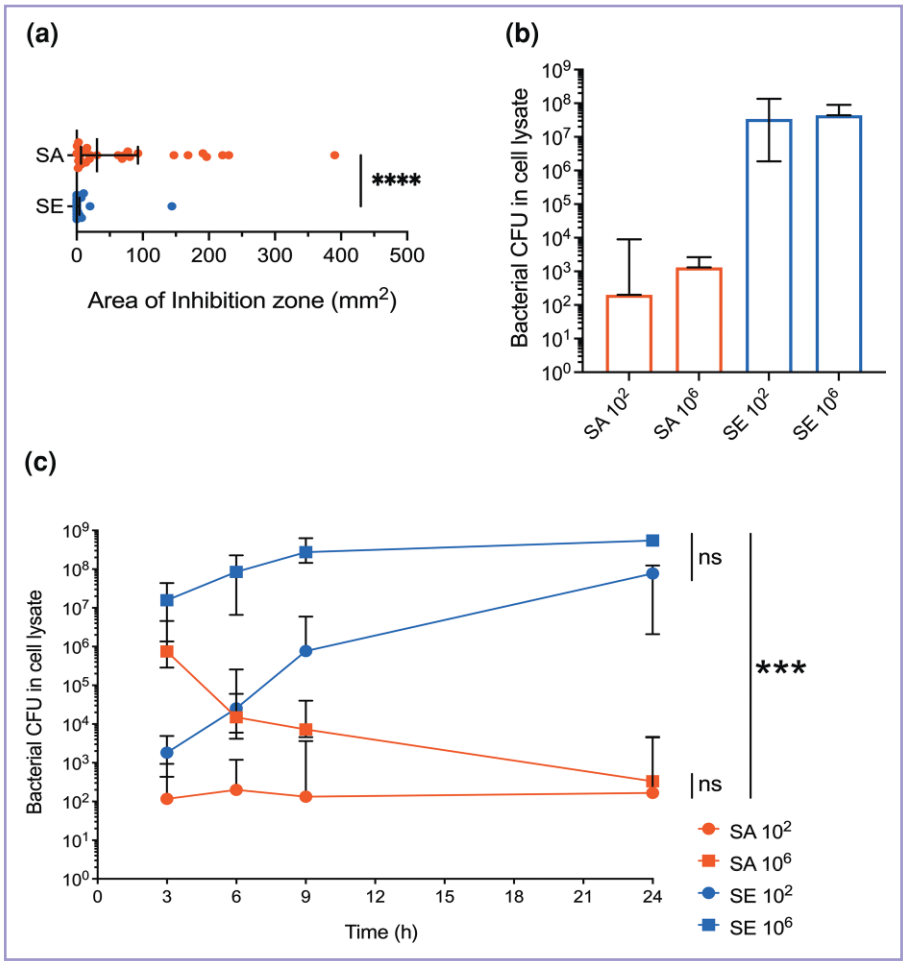

Figure 2 Colonization of epidermal models by staphylococcal species. (a) Calculated area of inhibition from explant human skin from five donors ($n=3$ or 6 per donor). 10^6 colony-forming units (CFU) of *Staphylococcus aureus* (SA) or *Staphylococcus epidermidis* (SE) suspended in 100 μL phosphate-buffered saline were spread onto agar plates to form bacterial lawns. Shown are the means with individual datapoints for each biopsy replicate. The inhibition zone was calculated by subtracting the biopsy size (8 mm) from the gross inhibited area (Figure S1b). Mann–Whitney test for significance: ****$P<0{\cdot}0001$. (b) Models in duplicate or triplicate were infected with either 10^2 or 10^6 colony-forming units (CFU) of SA or SE initially for 3 h to establish adherent or intracellular infection and were left in culture for a further 21 h. Bacteria were quantified by enumeration after serial dilution and plating on trypticase soy agar plates for colony counting after overnight incubation. Data are expressed as the mean and SD. (c) Time course of colonization of models by SA (red) and SE (blue) over 24 h at low (10^2 CFU, circles) and high (10^6 CFU, squares) inoculation loads at the indicated timepoints ($n=4$). Tests for statistical significance within species comparisons across challenge loads were performed by Kruskal–Wallis tests, and comparisons of across-species significance independent of challenge load were performed by Mann–Whitney tests. ***$P<0{\cdot}001$; ns, not significant.

and SA-challenged models. Genes expressed characteristically in basal (40% of cells), spinous (9.7%) and granular (50.2%) keratinocytes were used as markers to identify stratification (Figure 4a).

Density clustering by bacterial challenge demonstrated clear pathogen-specific differences in keratinocyte transcriptomes (Figure 4b). Considering individual epidermal strata, within these, transcriptomic subclustering was highly correlated with challenge conditions for both basal and spinous populations, but not granular keratinocytes (Figure 4c). These challenge-related strata subpopulations were further confirmed by unbiased clustering using the Leiden algorithm,[25] indicating the existence of transcriptome-based substratification within each layer independent of the proliferation–differentiation axis (Figure 4d). This suggests that the pathogen-induced subclustering within epidermal strata was not a result of keratinocyte differentiation and may be reversible.

Staphylococcus aureus challenge of epidermal models induces a specific spinous keratinocyte subpopulation

Based on *KRT1* and *KRT10* expression and challenge-annotated density plotting of UMAP projections, we considered Spinous-1 (S1) to represent a challenge-naive cluster, Spinous-2 (S2) an SE-related cluster, and Spinous-3 (S3) an SA-associated cluster (Figure 4d). Furthermore, visualization of an epidermal differentiation score across the whole dataset indicated that S3 highly expressed differentiation markers (Figure 5a).

We performed differential gene expression analysis comparing these three clusters (Figure 5; and Figure S4; see Supporting Information). In total, eight genes distinguished naive and SE spinous clusters, including canonical spinous markers *KRT1* and *KRT10*, which are found to be downregulated in S2 keratinocytes (Figure 5b, c).

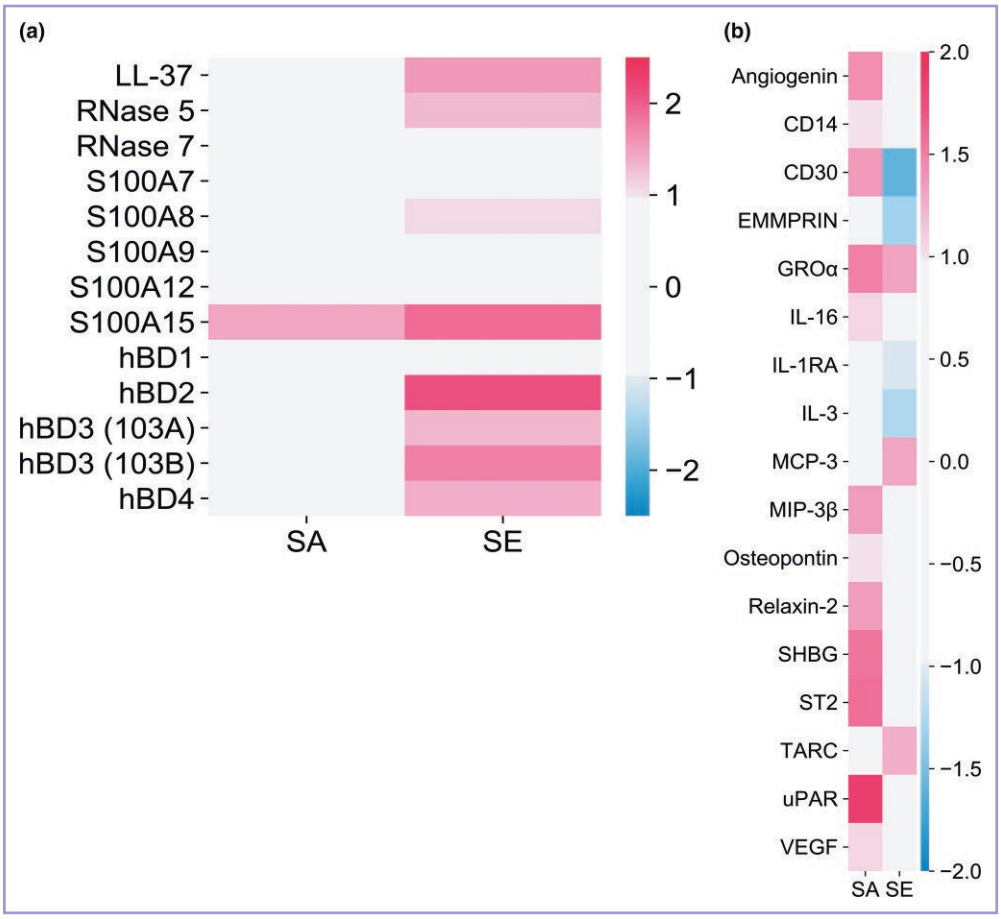

Figure 3 Secreted protein and cellular gene expression of keratinocytes induced by *Staphylococcus aureus* (SA) or *Staphylococcus epidermidis* (SE) colonization. (a) Heatmap of antimicrobial peptide gene expression from models colonized with staphylococcal species at 3 h and 24 h expressed as a relative $\log_2$ fold change vs. control models ($n=3$ or 4). (b) Heatmap of expressed analytes secreted in response to staphylococcal colonization of reconstituted human epidermis models. The Proteome Profiler Human XL Cytokine Array Kit was used to analyse expression of analytes in culture undernatants harvested from models infected with 10^6 colony-forming units of SA or SE and phosphate-buffered saline control after 24 h. Colonizations were performed in triplicate, with undernatant pooled for analyte analysis over two independent experiments (average of duplicate experiments shown). Expression was measured using ImageJ to determine the average relative spot intensity between two spots per analyte. Analyte expression is shown as $\log_2$ fold change relative to the control, showing only those analytes that were significant for SA and/or SE comparisons (full heatmap available in Figure S3).

However, SA-exposed keratinocytes from the S3 cluster, compared with the naive and SE spinous clusters, upregulated 27 (Figure 5e) and 26 (Figure 5g) genes, respectively (Figure S4). Of these, 19 were common between comparisons, and suggested activation of antimicrobial humoral responses (Gene Ontology: 0019730; Benjamini–Hochberg adjusted P-value $= 8.7 \times 10^{-7}$) and epidermis development (Gene Ontology: 0008544, Benjamini–Hochberg adjusted P-value $= 2.5 \times 10^{-6}$). SA-exposed keratinocytes, compared with naive cultures, also induced striking markers of inflammation, with upregulation of *CD24*, *IL1RN*, *SERPINB1* and *NEAT1*.[27–31] This indicated that the genes upregulated by SA challenge are unique to pathogenic challenge rather than general microbial colonization. Comparison between SA- and SE-exposed keratinocytes revealed the role of SA in upregulation of epidermal differentiation complex (EDC) genes such as *IVL* and *SPRR1B*; associated barrier genes including *DMKN*, *KRT6B* and *SBSN*; and the antimicrobial serpin *SERPINB3* (Figure 5g).

Bacterial challenge induces two distinct basal keratinocyte populations

Basal keratinocytes from each challenge could be assigned to two of four clusters. Basal-1 and Basal-2 (B1 and B2) were evident in unchallenged naive conditions. SE-challenged models induced Basal-2 and Basal-3 (B3), whereas SA also contributed to B3, and additionally Basal-4 (B4) (Figure 4c, d).

MAST differentially expressed gene analysis showed that SE did not induce any significant alteration in the transcriptome compared with the naive control (B2 vs. B1) (Table S1; see Supporting Information). In contrast, B3 (shared between SE and SA) induced a greater basal keratinocyte wounding response than B1 (Gene Ontology: 009611) (Benjamini–Hochberg adjusted P-value $= 0.026$) (Figure 6a; and Figure S5; see Supporting Information).

The B4 cluster was highly associated with SA challenge. The basal biology of these B4 keratinocytes was disturbed, as shown by reduced mRNA expression of basal *KRT5* and *KRT14*, alongside reduced *CXCL14* compared with naive B1

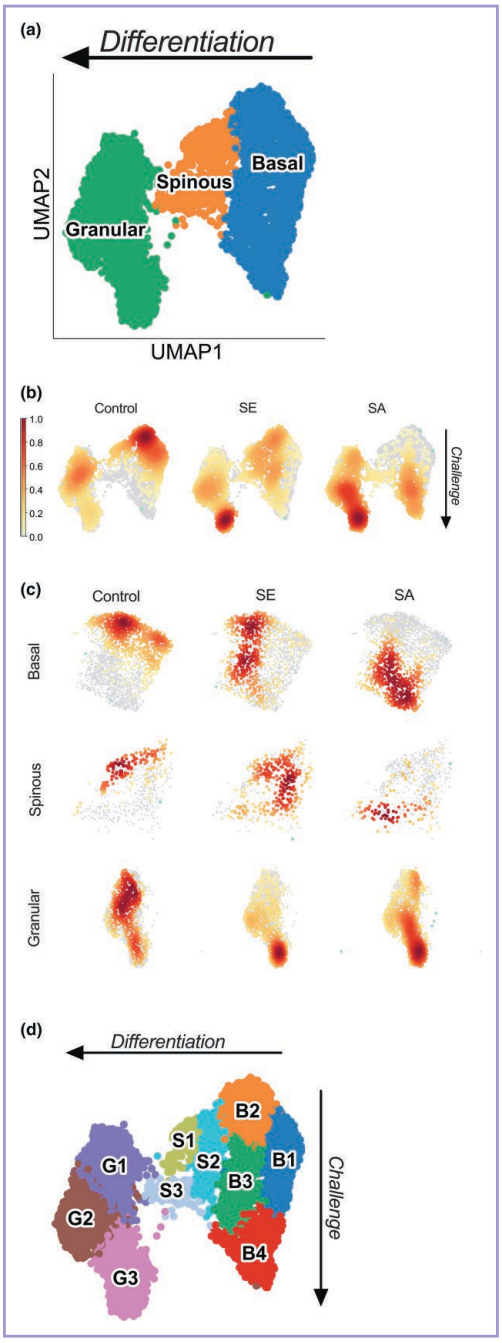

Figure 4 Clustering of single-cell RNA sequencing of keratinocytes from bacteria-challenged epidermal models. (a) Uniform Manifold Approximation and Projection (UMAP) of 6391 keratinocytes from epidermal models left as a microbe-naive control or challenged with *Staphylococcus aureus* (SA) or *Staphylococcus epidermidis* (SE). Differentiation layers were defined using unbiased Leiden clustering at a resolution of 0·2, which matched the approximate expression of canonical layer-defining markers. (b) The UMAP projection was coloured by embedded density according to challenge conditions: microbe naive (left), SE (middle) and SA (right), showing keratinocytes clustering from the same challenge condition by regions of more intense colour. (c) Embedded density plotting on the UMAP projection for separate basal (top), spinous (middle) and granular (bottom) layers according to challenge conditions: microbe naive (left), SE (middle) and SA (right). (d) Highly granular clustering to define keratinocyte stratification (basal, B; spinous, S; granular, G) and challenge-related subpopulations (numbered) defined by unbiased Leiden clustering at a resolution broadly matching the observations in (a) and (c).

cells (Figure 6b). Transcriptomic changes compared with naive basal keratinocytes (B1) showed downregulation of intermediate filament formation of the basal cytoskeleton (*KRT5*, *KRT14*, *KRT6A*, *KRT17*, *CXCL14* and *DST*), and upregulation of matrix metalloproteinase genes (*MMP1*, *MMP9* and *MMP10*) and laminin genes (*LAMA3*, *LAMB3* and *LAMC2*) in B4 keratinocytes (Figure 6c). These transcripts were not upregulated in the B3 populations, indicating their involvement in epidermal perturbation specific to SA. In addition, B4 cluster keratinocytes upregulated both immediate and delayed-release alarmins, IL-1α and IL-1β, indicative of attempted proinflammatory activation of other potential cutaneous populations of the epidermis.

Discussion

Staphylococci help govern cutaneous microbiome composition and are key species colonizing human skin.[32,33] Single-cell analysis of our models revealed stratified responses to microbial challenge. The stratified morphology describes the classical epidermal layers but also compartmentalizes proliferation and differentiation functions, tissue homeostasis and inflammation. Although this anatomy is well described, its contribution to epidermal homoeostasis and function is not yet fully understood.

Recent studies have used single-cell analysis to investigate this question; however, these are almost exclusively focused on the role of nonkeratinocyte inflammatory and immune populations underscoring epidermal heterogeneity.[34,35] The compartmentalization of processes involved in transcriptional programming of intercellular communication, inflammatory regulation and, particularly, follicular WNT signalling across healthy and inflamed epidermis from various anatomical sites has also recently been described.[17] Here the authors showed that almost one-eighth of the epidermal transcriptome aligns with classical differentiation patterns, yet their cutaneous function and biological mechanisms are unknown. This confirmed the utility of a single-cell approach to classify keratinocyte biology. However, it did not explore the effect of biologically relevant variables on keratinocyte differentiation, as we report.

We investigated the response of keratinocytes in a three-dimensional model to topical SE/commensal or SA/pathogen challenge by bulk and single-cell transcriptomic analysis and secreted protein factors. This identified an involucrin-expressing spinous population that was almost unique to SA-challenged epidermal models. Previously, it was demonstrated that differentiated involucrin-positive keratinocytes are critical to epidermal microbial regulation.[36] We demonstrate that SA growth was strongly inhibited, but SA challenge did not upregulate hBD2 expression, reported as a key protective factor released by keratinocytes against SA proteases.[37]

We postulate that through coevolutionary mechanisms, host surveillance against SA is highly sensitive and is activated by low bacterial load. The reason for this is likely facilitation of bacterial clearance before adverse infection occurs. Early SA clearance is necessary to prevent reaching a tipping point that leads to microbiome disruption, preferential overgrowth of SA and loss of cutaneous microbial diversity. Indeed, SA-induced dysbiosis is a key driver of cutaneous

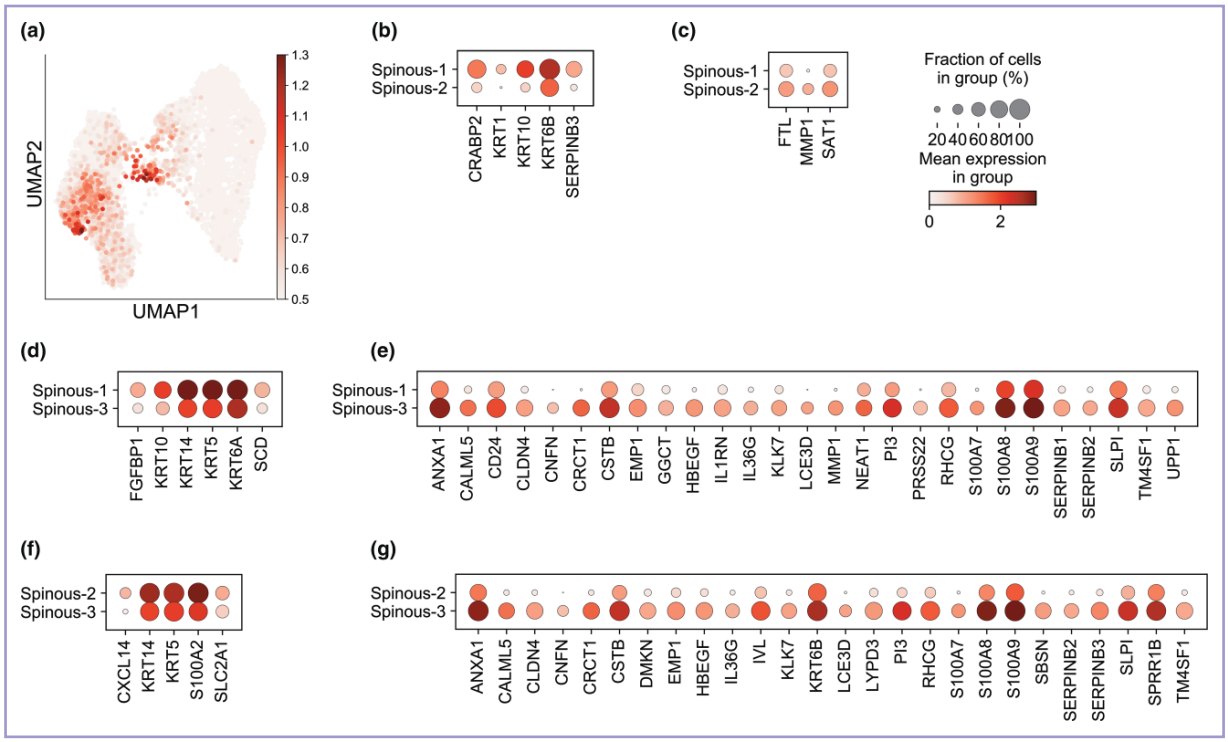

Figure 5 Gene expression of spinous keratinocytes. (a) Expression score for the panel of epidermal differentiation complex genes across the whole single-cell dataset represented in the Uniform Manifold Approximation and Projection (UMAP) space. (b) Differentially expressed genes (DEGs) upregulated in Spinous-1 cluster compared with Spinous-2. (c) DEGs upregulated in Spinous-2 cluster compared with Spinous-1. (d) DEGs upregulated in Spinous-1 cluster compared with Spinous-3. (e) DEGs upregulated in Spinous-3 cluster compared with Spinous-1. (f) DEGs upregulated in Spinous-2 cluster compared with Spinous-3. (g) DEGs upregulated in Spinous-3 cluster compared with Spinous-2. Statistical significance for differential expression within the MAST algorithm was defined as a Benjamini–Hochberg adjusted *P*-value < 0·01, |logFC| > 1.

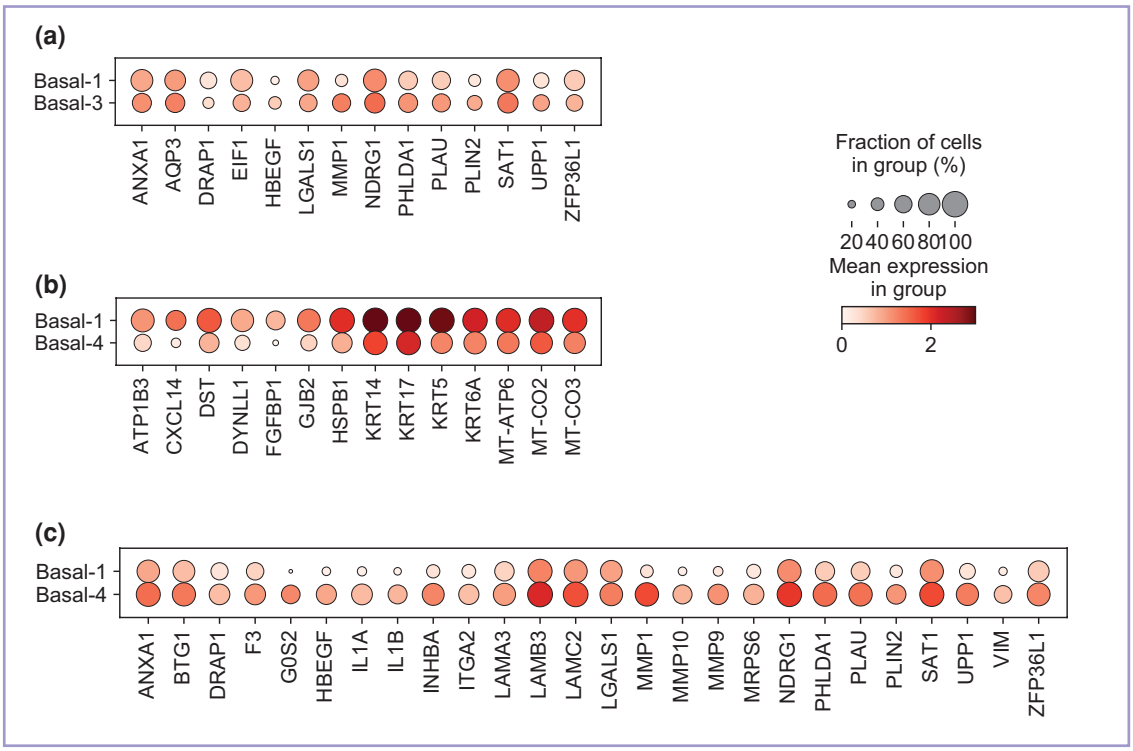

Figure 6 Gene expression of basal keratinocytes. (a) Differentially expressed genes (DEGs) upregulated in Basal-3 cluster compared with Basal-1. (b) DEGs upregulated in Basal-1 cluster compared with Basal-4. (c) DEGs upregulated in Basal-4 cluster compared with Basal-1. Statistical significance for differential expression within the MAST algorithm was defined as a Benjamini–Hochberg adjusted *P*-value < 0·01, |logFC| > 1.

inflammation in atopic eczema.[38] Our keratinocyte-only model demonstrates that, without the presence of the classical immune system, keratinocytes can inhibit SA growth, proving advantageous in preventing established colonization before other immune populations are recruited. It is plausible that this SA clearance begins soon after colonization, and expression of effector keratinocyte-derived AMPs is not captured at the timepoint we investigated. In contrast, colonization with SE primes the epidermis to expression of AMPs, in what can be considered a symbiotic relationship between host and bacteria to prevent colonization of pathogens.

We also show that spinous keratinocytes are sensitive to SA challenge. At the gene expression level, this population was characterized by inflammatory signalling. Interestingly, we saw that SE challenge induced much higher expression of hBD2, yet our data and other microbiological studies[37] confirmed that this did not inhibit SE growth. The SA-induced spinous population demonstrated greater expression of members of the IL-1 signalling pathway (*IL36G*, *IL1RN*, S100 genes). Wanke *et al.* reported that keratinocyte responses to SA infection via AMP release were dependent on IL-1 signalling.[36] Our data suggest that this IL-1 signalling arises in a distinct basal proliferating population induced by SA, also marked by overexpression of matrix metalloproteinase and laminin genes. Alternatively, sample timing may reflect a time course of bacterial responses across the stratified model, with those cells close to the apical surface demonstrating later AMP responses, and basal cells initiating earlier IL-1 responses to initiate AMP expression in this layer.

In the context of the whole epidermis, such IL-1-expressing basal cells will also provide danger signals to and prime other cutaneous immune populations, such as antigen-presenting cells. In the epidermis, IL-1α is constitutively expressed as a biologically inactive precursor for immediate release from keratinocytes upon receptor activation. Release of pro-IL-1α readily occurs during tissue trauma and infection to act as a damage-associated molecular pattern and is a potent trigger of IL-6 and tumour necrosis factor-α expression.[39] In contrast, IL-1β is a later proinflammatory mediator in response to pathogenic stimulation.[40] Our results indicated that SA pathogenic infection of the epidermis induced basal keratinocyte IL-1α release, accompanied by IL-1β as early as 24 h postchallenge. Therefore, this shift in basal biology is rapid but distinct from epidermal differentiation processes and potentially reversible. Reversal of such inflammatory alarmin responses, especially when arising inappropriately, might aid in restoring cutaneous homeostasis.

Basal keratinocyte responses to SA challenge were not homogeneous. Approximately 60% of basal cells from the SA-challenged models expressed alarmin and tissue remodelling genes. The precise reason for subclusters within an epidermal compartment is not clear, but may reflect yet unknown keratinocyte differentiation pathways or other regulatory factors. Spatial and temporal investigation of these subpopulations will help determine whether the proinflammatory response represents a population constitutive to basal lineage (i.e. all basal keratinocytes can experience this phenotype) during pathogen challenge, or whether it is a distinct and transient subset arising in response to pathogen challenge.

One of the limitations of this work is the model system, which relies on pure keratinocytes. However, we specifically chose this system so that we could characterize the keratinocyte compartment in detail in a differentiated model. Our *in vitro* differentiated keratinocyte models are not a full recapitulation of human epidermis, but do compose the major basal, differentiating and cornified layers of the tissue necessary for investigating stratified responses to bacterial challenge. Addition of skin-resident T cells and dendritic cells, as well as extension of the model to contain full-thickness dermis, would be beneficial, but such mixed-cell skin models remain a challenge. Further, while our study presents differences between SE and SA, future work should explore staphylococcal strain-specific regulation of the epidermal transcriptome.

In summary, we have investigated keratinocyte responses in the context of commensal or pathogenic challenge of an organotypic epidermal model. These data from bulk transcriptomic investigation have shown that keratinocyte AMP expression on challenge with SE is increased without adverse effects on bacterial growth, unlike in SA-challenged models. Single-cell investigation further established that SA-challenged models express defensins from an inflammatory spinous population, whereas IL-1 alarmin signalling arose from basal cells. Therefore, we propose that epidermal microbial responses induce compartmentalized responses in the epidermal strata, which in turn regulate the host inflammatory responses and modify antimicrobial mediator expression. Our microbiota response signatures may be useful in correlating clinical immune and microbiome endotypes to elucidate lesion aetiology and guide tailored therapy. Further molecular and spatial investigation of these populations may help to elucidate their specific role in inflammatory cutaneous diseases associated with microbiome dysbiosis such as atopic eczema, and could offer new therapeutic targets.

Acknowledgments

Our first thanks go to the patients who donated material for inclusion into our study. We also thank our funding bodies the Medical Research Council and Wellcome Trust, and the iCASE PhD studentship sponsor, Unilever, for providing the resources to undertake this research. For previous discussions and contributions, we are grateful to Rebecca Ginger, previously of Unilever (Colworth, UK). We acknowledge the use of the Iridis High Performance Computing Cluster (Iridis 4, University of Southampton, UK).

Funding sources

This work was supported by the Medical Research Council DTP PhD Scheme and iCASE partnership with Unilever (scheme no. MR/N014308/1). M.E.P. is funded by the Wellcome Trust (Sir Henry Dale Fellowship, Wellcome Trust grant no. 10937/Z/15/Z).

Conflicts of interest

The authors declare they have no conflicts of interest.

Data availability

Sequencing data for the microarray and single-cell RNA sequencing are stored in the Gene Expression Omnibus database, submission numbers GSE192454 and GSE192641, respectively.

Ethics statement

Explant skin tissue was donated from discard surgery and was consented under ethical approval (LREC number 07/Q1704/46).

References

1 Eckhart L, Lippens S, Tschachler E, Declercq W. Cell death by cornification. *Biochim Biophys Acta* 2013; **1833**:3471–80.
2 Ardern-Jones MR, Black AP, Bateman EA, Ogg GS. Bacterial superantigen facilitates epithelial presentation of allergen to T helper 2 cells. *Proc Natl Acad Sci U S A* 2007; **104**:5557–62.
3 Klicznik MM, Szenes-Nagy AB, Campbell DJ, Gratz IK. Taking the lead – how keratinocytes orchestrate skin T cell immunity. *Immunol Lett* 2018; **200**:43–51.
4 Nickoloff BJ, Turka LA. Immunological functions of non-professional antigen-presenting cells: new insights from studies of T-cell interactions with keratinocytes. *Immunol Today* 1994; **15**:464–9.
5 Naik S, Bouladoux N, Linehan JL *et al.* Commensal–dendritic-cell interaction specifies a unique protective skin immune signature. *Nature* 2015; **520**:104–8.
6 Lai Y, Di Nardo A, Nakatsuji T *et al.* Commensal bacteria regulate toll-like receptor 3-dependent inflammation after skin injury. *Nat Med* 2009; **15**:1377–82.
7 Li D, Wang W, Wu Y *et al.* Lipopeptide 78 from *Staphylococcus epidermidis* activates β-catenin to inhibit skin inflammation. *J Immunol* 2019; **202**:1219–28.
8 Eriksen NHR, Espersen F, Rosdahl VT, Jensen K. Carriage of *Staphylococcus aureus* among 104 healthy persons during a 19-month period. *Epidemiol Infect* 1995; **115**:51–60.
9 Bitschar K, Wolz C, Krismer B *et al.* Keratinocytes as sensors and central players in the immune defense against *Staphylococcus aureus* in the skin. *J Dermatol Sci* 2017; **87**:215–20.
10 Lai Y, Cogen AL, Radek KA *et al.* Activation of TLR2 by a small molecule produced by *Staphylococcus epidermidis* increases antimicrobial defense against bacterial skin infections. *J Invest Dermatol* 2010; **130**:2211–21.
11 Guzik TJ, Bzowska M, Kasprowicz A *et al.* Persistent skin colonization with *Staphylococcus aureus* in atopic dermatitis: relationship to clinical and immunological parameters. *Clin Exp Allergy* 2005; **35**:448–55.
12 Macosko EZ, Basu A, Satija R *et al.* Highly parallel genome-wide expression profiling of individual cells using nanoliter droplets. *Cell* 2015; **161**:1202–14.
13 Bæk KT, Frees D, Renzoni A *et al.* Genetic variation in the *Staphylococcus aureus* 8325 strain lineage revealed by whole-genome sequencing. *PLOS ONE* 2013; **8**:e77122.
14 MacLea KS, Trachtenberg AM. Complete genome sequence of *Staphylococcus epidermidis* ATCC 12228 chromosome and plasmids, generated by long-read sequencing. *Genome Announce* 2017; **5**:e00954-17.
15 Newman AM, Liu CL, Green MR *et al.* Robust enumeration of cell subsets from tissue expression profiles. *Nat Methods* 2015; **12**:453–7.
16 Clayton K, Vallejo A, Sirvent S *et al.* Machine learning applied to atopic dermatitis transcriptome reveals distinct therapy-dependent modification of the keratinocyte immunophenotype. *Br J Dermatol* 2021; **184**:913–22.
17 Cheng JB, Sedgewick AJ, Finnegan AI *et al.* Transcriptional programming of normal and inflamed human epidermis at single-cell resolution. *Cell Rep* 2018; **25**:871–83.
18 Stoeckius M, Zheng S, Houck-Loomis B *et al.* Cell Hashing with barcoded antibodies enables multiplexing and doublet detection for single cell genomics. *Genome Biol* 2018; **19**:224.
19 Sirvent S, Vallejo AF, Davies J *et al.* Genomic programming of IRF4-expressing human Langerhans cells. *Nat Commun* 2020; **11**:313.
20 Vallejo AF, Davies J, Grover A *et al.* Resolving cellular systems by ultra-sensitive and economical single-cell transcriptome filtering. *iScience* 2021; **24**:102147.
21 Wolf FA, Angerer P, Theis FJ. SCANPY: large-scale single-cell gene expression data analysis. *Genome Biol* 2018; **19**:15.
22 Lun ATL, Riesenfeld S, Andrews T *et al.* EmptyDrops: distinguishing cells from empty droplets in droplet-based single-cell RNA sequencing data. *Genome Biol* 2019; **20**:63.
23 Lun ATL, Bach K, Marioni JC. Pooling across cells to normalize single-cell RNA sequencing data with many zero counts. *Genome Biol* 2016; **17**:75.
24 Polański K, Young MD, Miao Z *et al.* BBKNN: fast batch alignment of single cell transcriptomes. *Bioinformatics* 2020; **36**:964–5.
25 Traag VA, Waltman L, van Eck NJ. From Louvain to Leiden: guaranteeing well-connected communities. *Sci Rep* 2019; **9**:5233.
26 Finak G, McDavid A, Yajima M *et al.* MAST: a flexible statistical framework for assessing transcriptional changes and characterizing heterogeneity in single-cell RNA sequencing data. *Genome Biol* 2015; **16**:278.
27 Hui L, Yongxia Z, Zhili G, Jun G. Calcitriol inhibits keratinocyte proliferation by upregulating leukocyte elastase inhibitor (serpin B1). *J Dermatol* 2014; **41**:393–8.
28 Lundberg KC, Fritz Y, Johnston A *et al.* Proteomics of skin proteins in psoriasis: from discovery and verification in a mouse model to confirmation in humans. *Mol Cell Proteomics* 2015; **14**:109–19.
29 Tan Y, Zhao M, Xiang B *et al.* CD24: from a hematopoietic differentiation antigen to a genetic risk factor for multiple autoimmune diseases. *Clin Rev Allergy Immunol* 2016; **50**:70–83.
30 Zhang P, Cao L, Zhou R *et al.* The lncRNA Neat1 promotes activation of inflammasomes in macrophages. *Nat Commun* 2019; **10**:1495.
31 Martin P, Palmer G, Rodriguez E *et al.* Intracellular IL-1 receptor antagonist isoform 1 released from keratinocytes upon cell death acts as an inhibitor for the alarmin IL-1α. *J Immunol* 2020; **204**:967–79.
32 Otto M. Staphylococcus colonization of the skin and antimicrobial peptides. *Expert Rev Dermatol* 2010; **5**:183–95.
33 Percival SL, Emanuel C, Cutting KF, Williams DW. Microbiology of the skin and the role of biofilms in infection. *Int Wound J* 2012; **9**:14–32.
34 He H, Suryawanshi H, Morozov P *et al.* Single-cell transcriptome analysis of human skin identifies novel fibroblast subpopulation and enrichment of immune subsets in atopic dermatitis. *J Allergy Clin Immunol* 2020; **145**:1615–28.
35 Reynolds G, Vegh P, Fletcher J *et al.* Developmental cell programs are co-opted in inflammatory skin disease. *Science* 2021; **371**:eaba6500.
36 Wanke I, Steffen H, Christ C *et al.* Skin commensals amplify the innate immune response to pathogens by activation of distinct signaling pathways. *J Invest Dermatol* 2011; **131**:382–90.
37 Wang B, McHugh BJ, Qureshi A *et al.* IL-1β-induced protection of keratinocytes against *Staphylococcus aureus*-secreted proteases

is mediated by human β-defensin 2. *J Invest Dermatol* 2017; **137**:95–105.
38 Kobayashi T, Glatz M, Horiuchi K *et al.* Dysbiosis and *Staphylococcus aureus* colonization drives inflammation in atopic dermatitis. *Immunity* 2015; **42**:756–66.
39 Kim B, Lee Y, Kim E *et al.* The interleukin-1α precursor is biologically active and is likely a key alarmin in the IL-1 family of cytokines. *Front Immunol* 2013; **4**:391.
40 Dinarello CA. Overview of the IL-1 family in innate inflammation and acquired immunity. *Immunol Rev* 2018; **281**:8–27.

Supporting Information

Additional Supporting Information may be found in the online version of this article at the publisher's website.